AIP | Applied Physics Letters

Carbon-coated Magnéli-phase TinO2n−1 nanobelts as anodes for Li-ion batteries and hybrid electrochemical cells

Wei-Qiang Han and Xiao-Liang Wang

Citation: Appl. Phys. Lett. **97**, 243104 (2010); doi: 10.1063/1.3525369
View online: http://dx.doi.org/10.1063/1.3525369
View Table of Contents: http://apl.aip.org/resource/1/APPLAB/v97/i24
Published by the American Institute of Physics.

Carbon-coated Magnéli-phase Ti_nO_{2n-1} nanobelts as anodes for Li-ion batteries and hybrid electrochemical cells

Wei-Qiang Han[a] and Xiao-Liang Wang
Center for Functional Nanomaterials, Brookhaven National Laboratory, Upton, New York 11973, USA

(Received 8 October 2010; accepted 17 November 2010; published online 15 December 2010)

We describe a method for preparing carbon-coated Ti_9O_{17} nanowires using $H_2Ti_3O_7$ nanobelts as precursors to react with ethane and hydrogen at high-temperature. The carbon-coating layers play a key role in restraining the sintering growth of the core during the phase transformation from $H_2Ti_3O_7$ to Magnéli-phase Ti_nO_{2n-1}, and in retaining the morphology of nanobelts. We demonstrated that the initial reversible capacity of these Ti_9O_{17} nanobelts attained 182 mA h g^{-1}, a value even higher than the theoretical value of a-TiO_2 (167 mA h g^{-1}). Cyclic-voltammetry measurement supports the pseudocapacitive lithium-storage behavior of these Magnéli-phase Ti_9O_{17} nanobelts. Furthermore, the nanobelts exhibit high power density along with excellent cycling stability in their application as hybrid electrochemical cells. © *2010 American Institute of Physics*. [doi:10.1063/1.3525369]

Inexpensive, nontoxic stoichiometric titanium dioxide (TiO_2) is considered an attractive candidate as an anode for rechargeable lithium-ion batteries (LIBs) because it is an efficient, low-voltage intercalation host for lithium ions.[1–3] Among the TiO_2 polymorphs, anatase,[3–5] rutile,[6] brookite,[7] and bronze (TiO_2–B) (Ref. 1) were applied for LIBs.[2] Electronically, these TiO_2 phases are wide-band-gap nonconducting materials, whose characteristics limit their efficiency in energy storage. The Magnéli-phase Ti_nO_{2n-1} (where n is a number between 4 and 10), which comprises two-dimensional chains of octahedral TiO_2 with every *n*th layer missing oxygen atoms to accommodate the loss of stoichiometry, exhibits a high electronic-conductivity comparable to that of graphite.[8–10] Their other advantages are insolubility in acid and electrochemical stability; accordingly, they are used widely in gas sensors, for photoelectrolysis, and in lead-acid batteries and fuel cells.[9] Han *et al.*[10] prepared Ti_4O_7 fibers and Ti_8O_{17} nanowires mixed with such fibers, respectively, by heat-treating thick $H_2Ti_3O_7$ nanobelts under a hydrogen atmosphere at 1050 and 850 °C. Nevertheless, it is still a challenge to prepare pure Magnéli-phase Ti_nO_{2n-1} nanorods. GaN nanowires, reportedly, can be coated with a graphitic carbon layer by decomposing methane at 900 °C.[11] Here, we describe our route to synthesizing graphitic carbon-coated Magnéli-phase Ti_9O_{17} nanobelts using $H_2Ti_3O_7$ nanobelts as templates; we also exploit their application as anodes for Li-ion batteries and hybrid electrochemical cells.

The precursors of $H_2Ti_3O_7$ nanobelts were prepared by a procedure reported earlier.[10,12,13] The widths of the nanobelts range from 30 to 200 nm, and their thicknesses from 15 to 40 nm; their lengths are up to 10 μm. The as-grown white $H_2Ti_3O_7$ nanobelts were put into an alumina crucible, sited in the hot zone of a thermal chemical-vapor deposition furnace, under flowing ethane (50 SCCM) (SCCM denotes cubic centimeter per minute at STP) and hydrogen (100 SCCM) while raising the temperature from 25 to 950 °C in 20 min, and then closing off the ethane and holding the material at 950 °C for 2 h. Afterward, we collected the black product from the crucible. Using the same experimental conditions except only using hydrogen (without ethane) as the reaction gas, we obtained bare thick fibers of Ti_9O_{17} whose sizes are about several micrometers, similar to the previous reported Ti_4O_7 fibers.[13]

The electrode films for measuring cell performance consisted of Ti_nO_{2n-1}, carbon black (Super P Li, TIMCAL, Westlake, Oh), and a poly(vinylideneflouride) binder. For Magnéli Ti_9O_{17}, the composition was 70:20:10 (coated) and 54:36:10 (bare). Copper foils (0.025 mm thick, 99.8%, Alfa) served as the current collector. The electrolyte solution was 1.0 M $LiPF_6$ in ethylene carbonate/dimethyl carbonate (1:1 by volume, purchased from Novolyte, Cleveland, Oh). A 20 μm polyolefin microporous membrane (Celgard 2320, Charlotte, NC) served as the separator. We fabricated laminated 2032-type coin cells with electrode films/electrolyte-saturated separators/lithium foils (as the counterelectrode and reference-electrode, 0.75 mm thick, 99.9% metal basis, Alfa, Ward Hill, MA). The cells were cycled by a galvanostatic procedure and the voltage ranges were 0.5–3 V for the Magnéli samples, and the current applied was expressed as C/*n* (i.e., fully charge or discharge of the theoretical capacity in *n* hours).

For characterizing the performance of Ti_nO_{2n-1} as anode materials in hybrid electrochemical cells (HECs), we fabricated similar laminated 2032-type coin cells with electrode films/electrolyte-saturated separators/activated carbon electrodes. The carbon-electrode films consisted of activated carbon (Alfa, −20+50 mesh) and polyvinylidene fluoride binder with a weight composition of 90:10. The energy density was calculated as $E=(1/2)CV^2$, where C is the specific capacitance with respect to the TiO_2 mass and V is the voltage span. We determined the power density as $P=E/\Delta t_d$, in which Δt_d is the cathodic (discharge) scan-time.[14] Cyclic voltammetry was carried out at varying scan rates with the same coin cells. For hybrid electrochemical cells, the *CV* scan was between 0 and 2.5 V.

Figure 1(a) shows an x-ray diffraction (XRD) spectrum of the product. Its characteristic spectral peaks denote that the sample is triclinic Ti_9O_{17} (a=5.57, b=7.1, c=22.15 Å, α=97.1°, β=131.0°, γ=109.8°).[15] The SEM image [Fig.

[a]Electronic mail: whan@bnl.gov.

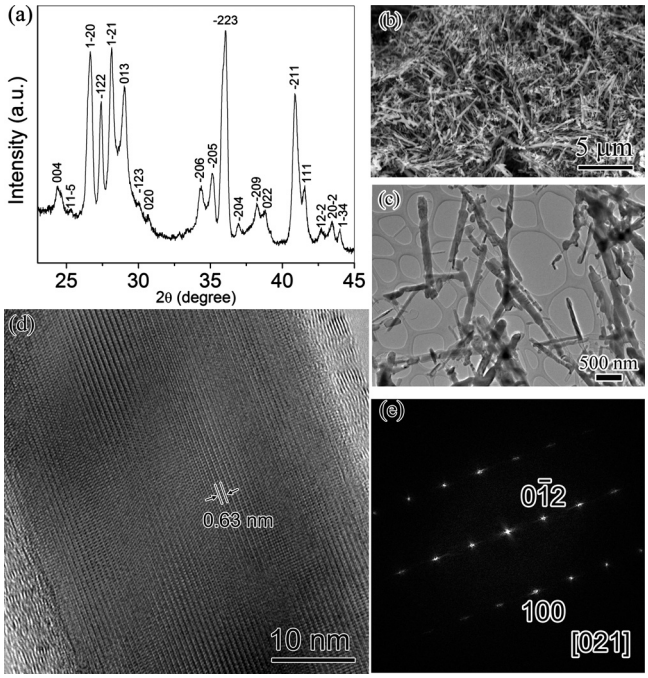

FIG. 1. (a) XRD spectrum of the carbon-coated Ti_9O_{17} nanobelts; (b) SEM image of the carbon-coated Ti_9O_{17} nanobelts; (c) a low-magnification TEM image of the carbon-coated Ti_9O_{17} nanobelts; (d) a high-magnification TEM image of a part of a carbon-coated single-crystal Ti_9O_{17} nanobelt; and (e) fast-Fourier transform electron-diffraction patterns of part of the Ti_9O_{17} nanobelt in (d).

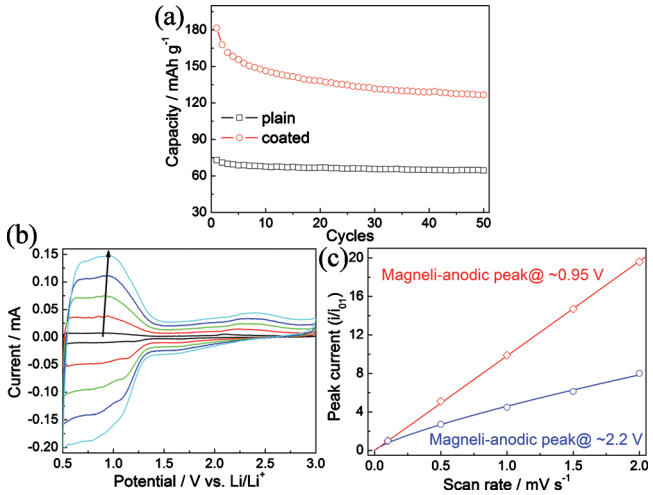

FIG. 2. (Color) (a) Reversible (Li^+ removal) capacities of coin cells with the carbon-coated Ti_9O_{17} nanobelts as the working electrodes and lithium metal as both the reference-electrode and counterelectrode. The cycling rate was C/10 based on theoretical capacity; (b) cyclic voltammograms of the carbon-coated Ti_9O_{17} nanobelts at scan rates of (along the arrows) 0.1, 0.5, 1, 1.5, and 2 mV s^{-1}; (c) normalized anodic peak-current with respect to the value at 0.1 mV s^{-1}, in which the lines are the fitted results.

1(b)] reveals that the samples are straight nanobelts, with smooth edges or not, and widths typically ranging from 30 to 200 nm, similar to the H_2Ti3O_7 nanobelts. Figure 1(c) is a low-magnification transmission electron microscopy (TEM) image of several nanobelts, again, they are straight ones. Figure 1(d) is a high-magnification TEM image of a part of a single-crystal nanobelt. The labeled distance is 6.3 Å, corresponding to the (01$\bar{2}$) plane of the triclinic mineral. The diameter of the nanobelt's core is 41 nm, and the thickness of the shell of the carbonlayers is 4.5 nm. The number of layers for different carbon-coated nanobelts typically ranges from 4 to 24, which is larger than that (1–5) of the carbon-coated GaN nanowires, in which fabrication methane, rather than ethane, was used.[11] The carbon-coating formed before the temperature reached 950 °C. This coating played a key role in suppressing the sintering growth of the core during the phase transformation from $H_2Ti_3O_7$ to the Magnéli-phase Ti_nO_{2n-1}, and kept intact the nanobelt's morphology. Figure 1(e) shows a fast-Fourier transform electron-diffraction pattern of part of the Ti_9O_{17} nanobelt depicted in Fig. 1(d). The weight ratio of the carbon coating of the product was characterized using a thermogravimetric analyzer. Thermogravimetric analysis measurement shows that the mass ratio of the carbon coating is about 16%.

As evident in Fig. 2(a), bare Magnéli Ti_9O_{17} fibers of several micrometers can deliver only a low capacity of about 70 mA h g^{-1}. However, most impressively, the reversible capacity jumps considerably in the graphite-coated sample. The value rises to about 182 mA h g^{-1} and stabilizes at 130 mA h g^{-1} after 50 cycles. We undertook cyclic-voltammetry characterization to understand Li-storage in the Ti_9O_{17} nanobelts. Figure 2(b) displays the voltammograms at varying scan rates (along the arrows) of 0.1, 0.5, 1, 1.5, and 2 mV s^{-1}. Each of them exhibits a pair of cathodic/anodic peaks with a formal potential of 0.9 V versus Li/Li^+ that is assignable to Ti_9O_{17}. The current response at lower voltages was attributed to electrolyte decomposition to form a solid electrolyte interface.[16] In Fig. 2(c), we compare the normalized anodic peak currents in cyclic voltammograms with the values obtained at the slowest scan rate of 0.1 mV/s. As demonstrated, for Ti_9O_{17} nanobelts, the currents of the main peaks at ~0.95 V scale with the first power of the scan rate, supporting a Faradaic pseudocapacitive charging-behavior,[17–20]

$$i = dQ/dt = CdU/dt = Cv, \quad (1)$$

where C is capacitance, v is the scan rate, and Q is the charge. The pseudocapacitive-storage mechanism in Ti_9O_{17} is reasonable, considering that the triclinic Magnéli-phase Ti_nO_{2n-1} lacks open structures in its lattices. Therefore, the Faradiac reaction occurring at the particles' surfaces mainly contributes to capacity. Accordingly, the special shape-feature of the nanobelt ensures that at least one of its dimensions is nanoscale, i.e., has a high surface area, and thus the Faradiac reaction can be processed efficiently and, consequently, a high capacity attained. By contrast, only a fraction volume of the bulk Ti_9O_{17} was at the surface and could involve in the Faradiac reaction; therefore, the capacity performance of bulk Ti_9O_{17} was relatively poor. Carbon coating is not only responsible for the morphology of Ti_9O_{17} nanobelts, but is also helpful in the enhancement of the Faradiac reaction because of its high electrical conductivity, which facilitates the transportation of charges associated with the reaction along the current pathway and results in the improvement of cell performance.[21]

The superior pseudocapacitive-storage behavior of C-coated Magnéli Ti_9O_{17} nanobelts makes it interesting to explore their application in HECs that integrate the high energy density of Li-incorporation anodes and the high power-density of electric-double-layer cathodes.[22,23] Here, we assembled and tested HECs with Ti_9O_{17} as the anode, and activated carbon as the cathode (Fig. 3). The shape of the cyclic voltammograms is distorted, deviating from the rect-

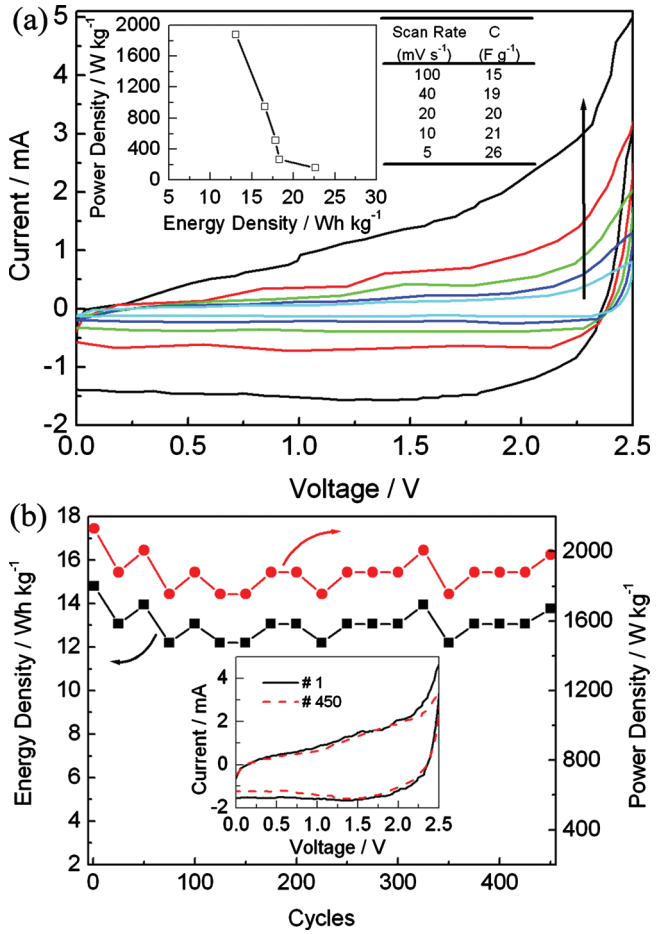

FIG. 3. (Color) (a) Cyclic voltammograms of the Ti_9O_{17}/activated carbon-cell at scan rates of (along the arrows) 5, 10, 20, 40, and 100 mV s^{-1}, where the inset figure shows the Ragone plot of power density vs energy density, and the inset table shows the capacitance; (b) cycling performance of the cell at 100 mV s^{-1}, where the inset shows the *CV* profiles at the first and 450th cycles.

angular shape of ideal carbon/carbon capacitors; this became more prominent with increasing scan rate due to the overlapping effect of the two different energy-storage mechanisms, viz., Li-insertion into Ti_9O_{17} and PF_6^--absorption onto carbon.[22,23] A specific cell-capacitance of 26 F g^{-1} was displayed at a scan rate of 5 mV s^{-1}, derived via Eq. (1) using the cathodic-(discharge) current at 1.25 V;[14,24] thus, an energy density of 23 W h kg^{-1} and a power density of 163 W kg^{-1} could be achieved. The merit of these HECs is seen in the Ragone plot [inset of Fig. 3(a)], where a power density as high as about 1900 W kg^{-1} was attainable, with an energy density higher than 10 W h kg^{-1}. Moreover, characteristically, the Ti_9O_{17}-carbon system has excellent cycling stability. After 450 cycles at 100 mV s^{-1}, the energy and power densities are well maintained, and the *CV* curves are almost identical [Fig. 3(b)]. The performance of this Ti_9O_{17}-carbon HEC is comparable to that reported for the TiO_2 (B) nanowire-carbon nanotube system.[22]

In summary, we developed an efficient way to prepare carbon-coated Ti_9O_{17} nanobelts. The initial reversible capacity of the Ti_9O_{17} nanobelts attained 182 mA h g^{-1}. Cyclic voltammetry reveals the pseudocapacitive lithium-storage behavior of Magnéli-phase Ti_9O_{17} nanobelts. They show high power-density with excellent cycling stability in their application as hybrid electrochemical cells.

This research was carried out at the Center for Functional Nanomaterials, Brookhaven National Laboratory (BNL), which is supported by the U.S. Department of Energy, Office of Basic Energy Sciences, under Contract No. DE-AC02-98CH10886, and the E-LDRD Fund of Brookhaven National Laboratory.

[1]A. R. Armstrong, G. Armstrong, J. Canales, R. Garcia, and P. G. Bruce, Adv. Mater. (Weinheim, Ger.) **17**, 862 (2005).
[2]Z. G. Yang, D. Choi, S. Kerisit, K. M. Rosso, D. H. Wang, J. Zhang, G. Graff, and J. Liu, J. Power Sources **192**, 588 (2009).
[3]J. S. Chen, Y. L. Tan, C. M. Li, Y. L. Cheah, D. Y. Luan, S. Madhavi, F. Y. C. Boey, L. A. Archer, and X. W. Lou, J. Am. Chem. Soc. **132**, 6124 (2010).
[4]R. J. Cava, D. W. Murphy, S. Zahurak, A. Santoro, and R. S. Roth, J. Solid State Chem. **53**, 64 (1984).
[5]C. L. Olson, J. Nelson, and M. S. Islam, J. Phys. Chem. B **110**, 9995 (2006).
[6]T. Ohzuku, Z. Takehara, and S. Yoshizawa, Electrochim. Acta **24**, 219 (1979).
[7]M. A. Reddy, M. S. Kishore, V. Pralong, U. V. Varadaraju, and B. Raveau, Electrochem. Solid-State Lett. **10**, A29 (2007).
[8]S. Andersson, B. Collen, U. Kuylenstierna, and A. Magneli, Acta Chem. Scand. (1947-1973) **11**, 1641 (1957).
[9]J. R. Smith, F. C. Walsh, and R. L. Clarke, J. Appl. Electrochem. **28**, 1021 (1998).
[10]W. Q. Han and Y. Zhang, Appl. Phys. Lett. **92**, 203117 (2008).
[11]W. Q. Han and A. Zettl, Adv. Mater. (Weinheim, Ger.) **14**, 1560 (2002).
[12]T. Kasuga, M. Hiramatsu, A. Hoson, T. Sekino, and K. Niihara, Adv. Mater. (Weinheim, Ger.) **11**, 1307 (1999).
[13]W. Q. Han, L. J. Wu, R. F. Klie, and Y. M. Zhu, Adv. Mater. (Weinheim, Ger.) **19**, 2525 (2007).
[14]W. Xing, S. Z. Qiao, R. G. Ding, F. Li, G. Q. Lu, Z. F. Yan, and H. M. Cheng, Carbon **44**, 216 (2006).
[15]JCPDF Card No. 018-1405.
[16]B. Scrosati and J. Garche, J. Power Sources **195**, 2419 (2010).
[17]M. Zukalová, M. Kalbáč, L. Kavan, I. Exnar, and M. Graetzel, Chem. Mater. **17**, 1248 (2005).
[18]J. Wang, J. Polleux, J. Lim, and B. Dunn, J. Phys. Chem. C **111**, 14925 (2007).
[19]T. Brezesinski, J. Wang, J. Polleux, B. Dunn, and S. H. Tolbert, J. Am. Chem. Soc. **131**, 1802 (2009).
[20]J. Jamnik and J. Maier, Phys. Chem. Chem. Phys. **5**, 5215 (2003).
[21]M. S. Whittingham, Chem. Rev. (Washington, D.C.) **104**, 4271 (2004).
[22]Q. Wang, Z. H. Wen, and J. H. Li, Adv. Funct. Mater. **16**, 2141 (2006).
[23]D. W. Wang, H. T. Fang, F. Li, Z. G. Chen, Q. S. Zhong, G. Q. Lu, and H. M. Cheng, Adv. Funct. Mater. **18**, 3787 (2008).
[24]L. Z. Fan, Y. S. Hu, J. Maier, P. Adelhelm, B. Smarsly, and M. Antonietti, Adv. Funct. Mater. **17**, 3083 (2007).